https://doi.org/10.1051/e3sconf/202451603003

Banana peels based zinc oxide doped silver nanoparticles for enhanced photocatalytic degradation of paracetamol

Mohamad Aizad Mohd Mokhtar[1], *Roshafima* Rasit Ali[1*], *Zhongfang* Lei[2], and *Zatil Izzah* Ahmad Tarmizi[1]

[1]Department of Chemical and Environmental Engineering, Malaysia-Japan International Institute of Technology, Universiti Teknologi Malaysia, Jalan Sultan Yahya Petra, 54100 Kuala Lumpur, Malaysia
[2]Faculty of Life and Environmental Sciences, University of Tsukuba, 1-1-1 Tennodai, Tsukuba, Ibaraki, 305-8527, Japan

Abstract. Paracetamol (PCM) is a common drug for daily use in each household and considering PCM's availability and huge production, traces of waste PCM present in water sources are concerned. Photocatalysis technology shows promising results with the utilization of semiconductor materials and light energy to degrade and remove organic pollutants. In this study, zinc oxide/silver nanoparticles (ZnO/Ag NPs) photocatalyst were synthesized via sol-gel and co-precipitation technique with the aid of banana peels extract (BPE) for photodegradation of PCM. The produced photocatalysts were characterized by Ultraviolet-Visible Spectroscopy (UV-Vis), X-ray Diffraction (XRD), surface area and pore analysis and Field Emission Scanning Electron Microscope (FESEM). Results shows that a blue shift phenomenon occurs between ZnO NPs and ZnO/Ag NPs while XRD analysis suggested that all samples exhibit hexagonal wurtzite structure. ZnO/Ag NPs portrayed a spherical and hexagonal surface morphology with average particles size of 25.68 nm and mesoporous structure. ZnO/Ag NPs shows the highest photodegradation of PCM with 96 % with five repeated cycles compared to pristine ZnO NPs. The main species responsible for PCM degradation via ZnO/Ag are hydroxyl radical and electron. The prepared BPE based ZnO/Ag has a high potential as advanced materials for pharmaceutical wastewater treatment.

1 Introduction

Emerging contaminants (EC) are organic compounds that adversely affect human health and the environment [1]. Water contaminant groups such as pharmaceutical compounds, pesticides, personal care products, hormones, disinfectants, preservatives, surfactants, plasticizers and heavy metals are categorized as EC [2, 3]. EC is in demand with high consumption and usage as the world population is growing, becoming water pollutants because of improper discharge and disposal from industries and municipal effluents [4]. Pharmaceutical contamination comes from various sources such as effluent from hospitals, pharmaceutical manufacturing, human excretion, improper drug disposal and intensive livestock farming [5]. Examples of pharmaceutical compound groups include antibiotics, analgesics, antiepileptics, anticoagulants and anti-inflammatories [6]. Paracetamol (PCM) are widely used as anti-inflammatory and analgesic drugs for human and animal medication [7]. It is also one of the world's top 200 drugs for pain relief usages such as headaches, muscular ache, backaches and joint pain [8]. However, high dosage of PCM may lead to human and animal liver failure, hepatic necrosis and death [9] when it converts to N-acetyl-p-benzoquinone imine via oxidation [10]. Several technologies have been applied to treat pharmaceutical waste, including the conventional method of filtration, adsorption, sedimentation, flocculation and biological treatment. However, these methods are unsuitable for removing pharmaceutical compounds because they will produce sludge that will act as secondary pollution and further treatment need to be applied [11]. In addition, many researchers are practicing and applying Advanced Oxidation Processes (AOPs) as they can give alternative solutions to degrade organic compounds [12]. AOPs are chemical treatments that utilise oxidation as low waste generation technology in removing organic compound effluents [13]. Several AOPs methods include photocatalysis, photolysis, hydrogen peroxide-based, ozone-based and Fenton-based [5]. Among AOPs available, photocatalysis works by producing an electron (e^-) and hole (h^+) pair from the phenomenon of e^- in the valence band (VB) of the semiconductor that will jump to the conduction band (CB) as a result of the irradiation of light sources with the final product of carbon dioxide (CO_2) and water (H_2O) [8, 3, 4]. Zinc oxide nanoparticles (ZnO NPs) is extensively used in photochemical applications since it is an n-type semiconductor that offers large exciton binding energy and wide band gap properties, which is suitable for photocatalytic activities [3]. Coupling ZnO with Ag nanoparticles (ZnO/Ag NPs) is a promising advanced material that several studies had previously reported for various applications such as antifungal [14], photocatalytic [15], anti-microbial [16] and sensor [17]. ZnO/Ag NPs can improve charge separation and

* Corresponding author: roshafima@utm.my

inhibition of e^- and h^+ pair recombination and enhancing photocatalytic properties [18]. Khan et al. [19] reported a green synthesized ZnO/Ag NPs using *Acacia arabica* plant leaves with spherical morphology and successfully degrading 90 % methylene blue dye with visible light. Meanwhile, Ahmad et al. [20] studied the activities of biogenic ZnO NPs and ZnO/Ag NPs using *Carya illinoinensis* with 75 % and 91 % degradation of rhodamine B dye respectively, indicating the enhanced photocatalytic performance of ZnO/Ag NPs. Green synthesis can promote eco-friendly techniques for large scale and ease of production [21]. It also acts as a modification technique in synthesizing nanomaterials in which different morphologies, porosity and surface area can be modified. Utilizing waste material such as banana peels is one of the techniques in the green synthesis method. In this study, ZnO NPs and ZnO/Ag NPs were synthesized and characterized with the aid of banana peels extract for photodegradation of paracetamol with reusability and radical scavenging analysis.

2 Materials and methods

Banana peels were collected from a farm in Selangor, Malaysia. Analytical grade of zinc nitrate hexahydrate ($Zn(NO_3)_2{\cdot}6H_2O$, 98 %), sodium hydroxide (NaOH, 97%) ethylenediaminetetraacetic acid (EDTA), dimethyl sulfoxide (DMSO) and isopropyl alcohol (IPA) were purchased from R&M Chemicals, Malaysia. Silver nitrate ($AgNO_3$, 99 %) was purchased from Fisher Scientific, Malaysia while commercial paracetamol (Brand Panadol, paracetamol 500 mg) was purchased from pharmacy. All aqueous solution were prepared using deionized water (DI water). The Ultraviolet-visible spectroscopy (UV-Vis) was used to observe the absorbance peaks of BPZ and ZnO/Ag in the range of 220 – 800 nm using the Shimadzu UV-2600 UV-visible spectrophotometer (Shimadzu, Japan). The X-ray diffraction (XRD) were carried out using the PANalytical X'pert PRO X-Ray diffractometer (Malvern Panalytical, United Kingdom) at 2θ (20 – 80°). The Field Emission Scanning Electron Microscope (FESEM) instrument model JEOL (JSM6330F) used the electron beam energy range from 0.5-30 kV with magnification range of 10 to 500000. The surface area and pore analysis were measured using the physisorption of nitrogen gas at 77 K via Quantachrome Instrument Novatouch. Before analysis, all samples were degassed for 2 h at 150 °C.

2.1 Preparation of banana peels extract

Banana peels were washed thoroughly with tap water and again with DI water before dried in oven for 24 h. The dried peels were crushed and stored at room temperature. To prepare banana peels extract (BPE), DI water was mixed with dried peels at 1:10 ratio at 60 ºC for 1 h. Then, the extract was filtered and centrifuged at 10,000 rpm for 5 min to remove impurities and stored at 4 ºC for further use in green synthesis of ZnO/Ag.

2.2 Green synthesis of ZnO/Ag

The prepared ZnO/Ag follows as reported by our previous study [22]. In short, 20 ml of BPE were mixed with 5 g of $Zn(NO_3)_2.6H_2O$ at 80 °C and stirred until a gel-like formation produced. Then, the gel was collected and calcined for 1 h at 600 °C. The produced, white-colored ZnO NPs powder was named BPZ. Replacing BPE with DI water by the same procedure, DIZ was produced as control. 1 g of prepared BPZ powder was dispersed in 0.005 and 0.007 M $AgNO_3$. Then, the mixture was sonicated for 30 min until homogenous. 20 ml of prepared BPE was mixed into the mixture with continuous stirring. Then, 0.5 M NaOH was mixed into the mixture to form a precipitate and stirred for 2 h at 60 °C. The precipitate was centrifuged, sonicated, and washed with DI water three times. Finally, the precipitate was collected and dried at 80 °C for 24 h. The produced ZnO/Ag powder was named as Z5A and Z7A and stored in dark at room temperature for further experiment.

2.3 Photocatalytic degradation of paracetamol

PCM solution of 20 ppm with an unchanged of pH value 6 were prepared beforehand. Initially, 0.1 g of synthesized BPZ and ZnO/Ag NPs was mixed with the PCM solution and sonicated for 5 min to ensure dispersion of ZnO/Ag NPs. Then, the mixture was placed in a photocatalytic reactor and stirred in the dark for 30 min to achieve absorption-desorption equilibrium monitored using UV-Vis. Next, 36-Watt UV light was turned on for 3 h with every 10 min sample was taken to be centrifuged and analysed using UV-Vis. The percentage degradation and rate constant were calculated using Eq. 1 and 2 where where C_0, C, $k_{apps,}$ and t are the initial concentration, final concentration, first-order kinetic rate constant, and reaction time.

$$\text{Degradation (\%)} = (C_o – C / C_o) \times 100\% \tag{1}$$

$$\ln (C_o / C_o) = k_{apps}t \tag{2}$$

3 Results and discussion

3.1 Formation of ZnO NPs and ZnO/Ag NPs

The green synthesized of BPZ, Z5A and Z7A was analysed and confirmed by UV-Vis spectroscopy in the range of 300 to 550 nm as shown in Fig. 1. The absorption peak of BPZ was detected around 368 nm while all Z5A and Z7A were detected in the lower range of wavelength around 365 nm. A bathochromic shift or blue shift phenomenon was observed which indicated the successful hybrid coupling formation of ZnO/Ag NPs. The blue shift was observed due to the electromagnetic interaction combination of Zn^{2+} and Ag^+ between adjacent colloidal nanoparticles [23]. Furthermore, the blue shift occurrence shows changes in the dielectric constant and size reduction in nanoparticles [24].

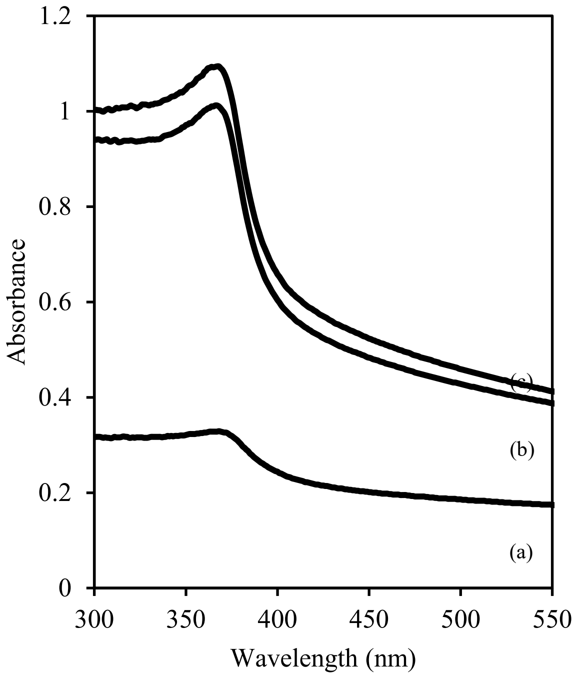

Fig. 1. UV-Vis spectra of (a) BPZ (b) Z7A and (c) Z5A

3.2 XRD analysis

The crystallographic structure of BPZ, Z5A and Z7A were determined using XRD analysis at 2θ within 20 – 80º as shown in Fig. 2. Diffraction peaks of hexagonal wurtzite phase of BPZ represented at 31.85º (100), 34.53º (002), 36.39º (101), 47.62º (102), 56.67º (110), 63.01º (103), 66.50º (200), 68.14º (112), 69.27º (201), 72.65º (004) and 77.14º (202) planes corresponded to JCPDS card no. 36-1451 [25]. After doping with Ag to produce ZnO/Ag NPs, samples of Z5A and Z7A had changes in the diffraction peaks with the addition of Ag in the secondary phase. The diffraction peaks of cubic phase Ag were observed at 38.13º (111) and 44.29º (200) planes corresponding to JCPDS card no. 2-109 [26].

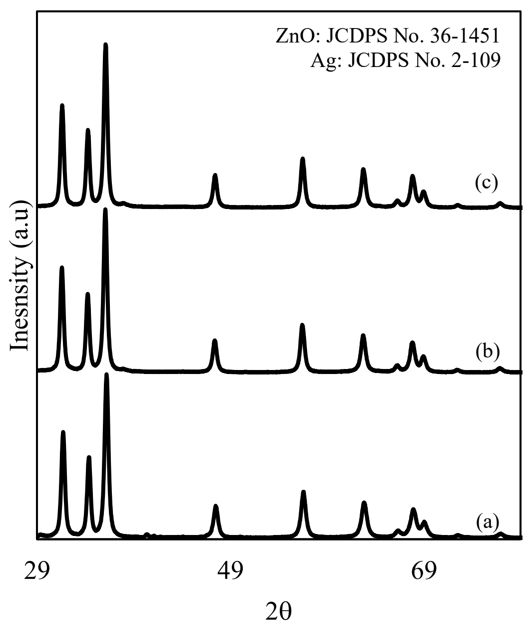

Fig. 2. XRD spectra of (a) BPZ (b) Z5A and (c) Z7A

3.3 Surface morphology analysis

The surface morphology and average size of the green synthesized Z7A using FESEM instrument since it had the highest photodegradation activity towards PCM. The result shows that Z7A shows morphologies of spherical and hexagonal in shape with no agglomeration phenomenon as shown in Fig. 3. The utilization of BPE as a capping agent in the synthesis of Z7A was demonstrated by the uniform particle size distribution [27] with average particle size of 25.68 nm. Z7A is smaller compared to the one in a previous study using the similar synthesis techniques reported by Thatikayala et al. [28] with an average size of 50-60 nm.

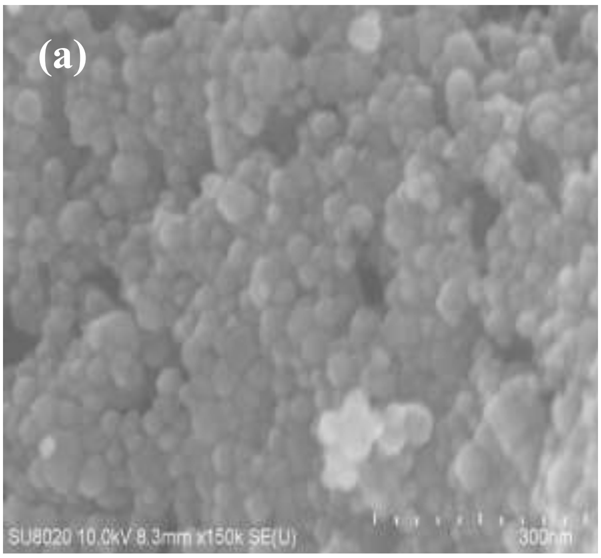

https://doi.org/10.1051/e3sconf/202451603003

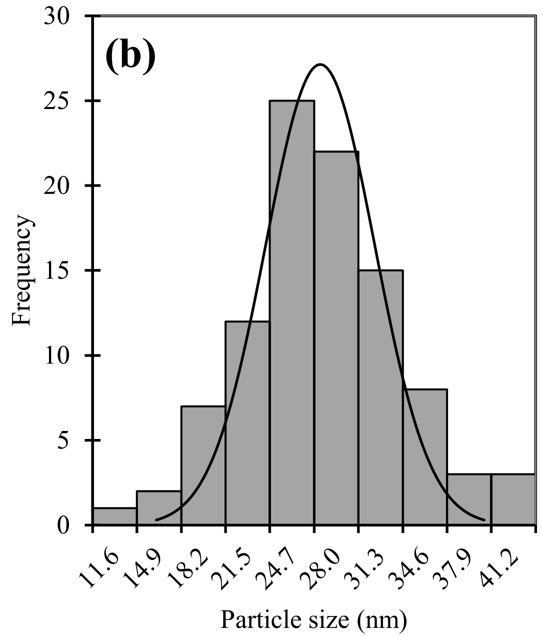

Fig. 3. (a) FESEM image and (b) size distribution of Z7A

3.4 Surface area and porosity analysis

The surface area and pore analysis of Z7A was determined using Quantachrome Instrument Novatouch. The Brunauer–Emmett–Teller (BET) and Barrett–Joyner–Halenda (BJH) model were used to calculate the surface area and pore volume respectively [29]. The BET surface area of Z7A is 13.524 m^2g^{-1} with pore volume of 0.044178 cm^3g^{-1}. Based on Fig. 4, the nitrogen adsorption-desorption isotherm can be classified as Type IVa indicating Z7A are mesoporous [30].

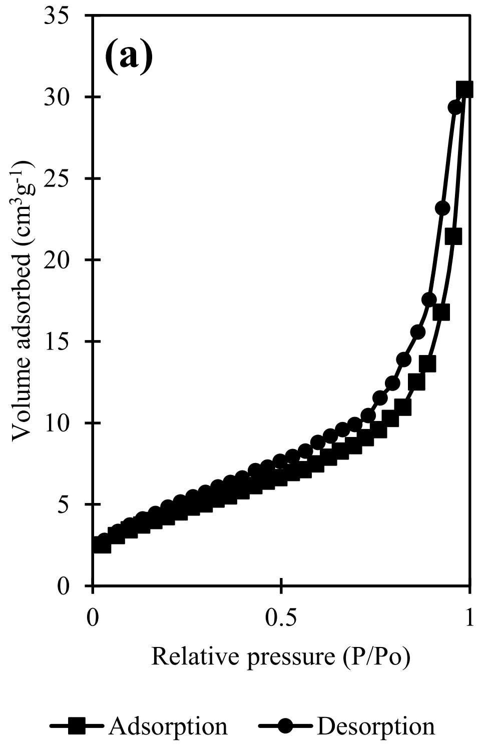

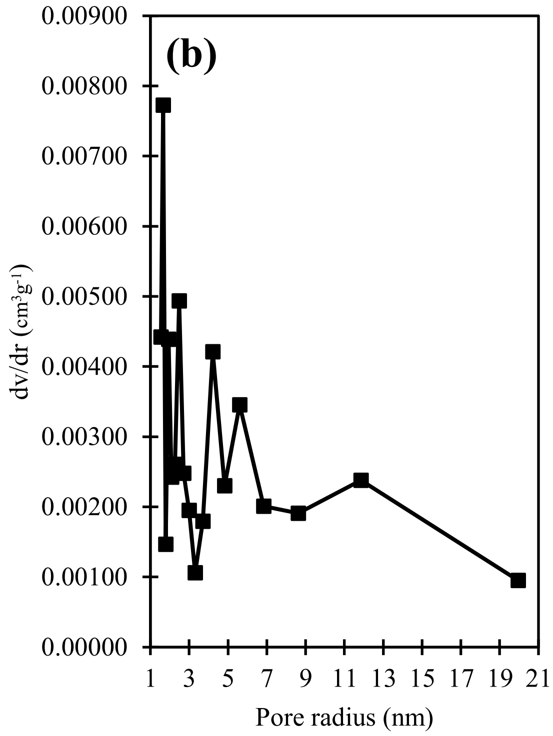

Fig. 4. (a) Nitrogen adsorption-desorption isotherms and (b) pore size distribution of Z7A

3.5 Effect of different photocatalyst and dosage on photodegration of paracetamol

Results show that BPZ has better performance compared to chemically synthesized DIZ as shown in Fig. 5a. which highlighted that green synthesis techniques can produce better photocatalysts [31]. Furthermore, among all ZnO/Ag NPs samples, Z7A has the highest PCM photodegradation of 96 % and 0.0173 min^{-1}. The introduction of Ag component in the composite plays a crucial role to inhibit electron-hole pair recombination through surface plasmon resonance [18]. The performance of Z7A is better compared to several previous studies using ZnO/Ag nanocomposite for PCM degradation. For example, Al-Gharibi et al. [32] reported to degrade at 92 % while Ramasamy et al. [18] degrade at 90.8 % of PCM. The effect of Z7A dosage towards photodegradation of PCM was studied at constant 20 ppm PCM concentration, pH 6 and 180 min. The dosage used was in the range of 00.5, 0.1, 0.15 and 0.2 g as shown in Fig. 5b. Results show that 0.1 g has the highest degradation percentage of 96 % compared to other amounts. Furthermore, increasing the dosage amount of Z7A shows decreasing in performance at 89 % and 64 % for 0.15 g and 0.2 g respectively.

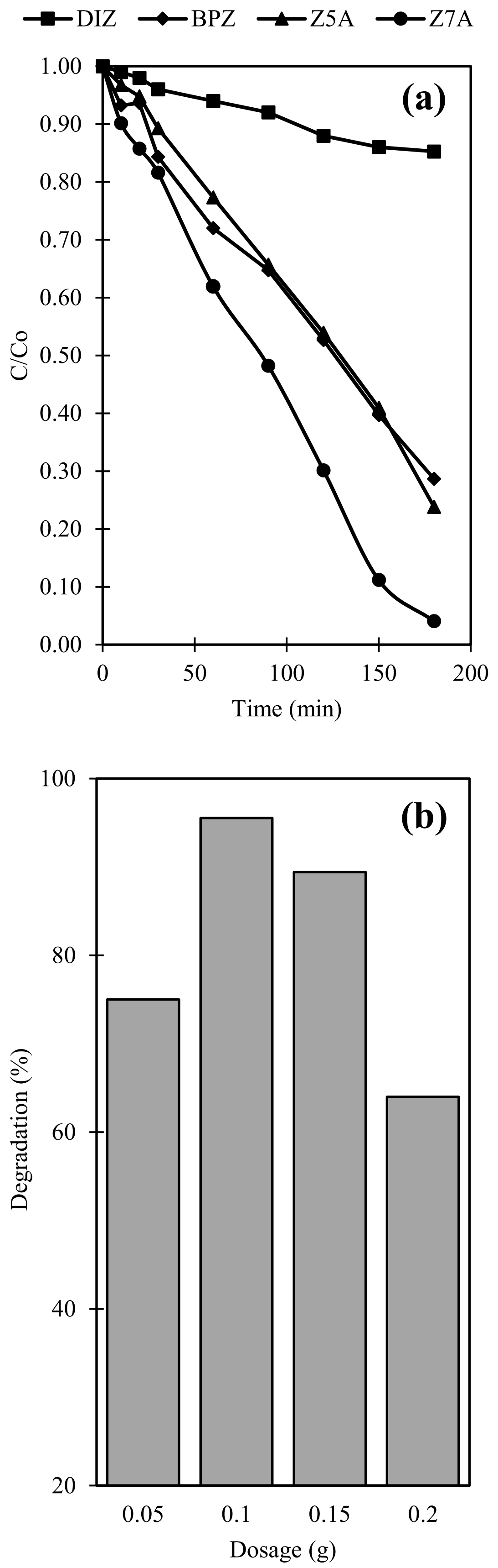

Fig. 5. Photodegradation of PCM using (a) various photocatalyst and (b) dosages (condition: time = 180 min and pH = 6)

3.6 Reusability and radical scavenging analysis

The reusability test was conducted using Z7A for five consecutive cycles. Based on Fig. 6a, the highest degradation percentage is in the first and second cycles which are 96 % and decreased to 92 %. Upon continuing the cycles, the degradation percentage decreased to 72 % for the last cycle. The reduction of degradation might be due to the loss of photocatalysts during the collection process. Overall, the reusability of Z7A shows above 60 % for all cycles indicating a high potential for reusability. The photocatalytic degradation mechanism of Z7A with PCM was studied using radical scavenging analysis. The scavengers that were used are EDTA, DMSO and IPA which act as photogenerated holes (h^+), photogenerated electrons (e^-) and hydroxyl radical (·OH) respectively. Based on Fig. 6b, the addition of EDTA, DMSO and IPA reduced the degradation percentage to 72 %, 13 % and 6 % respectively. From the analysis, results show that the main species responsible for PCM degradation via Z7A are ·OH and e^-.

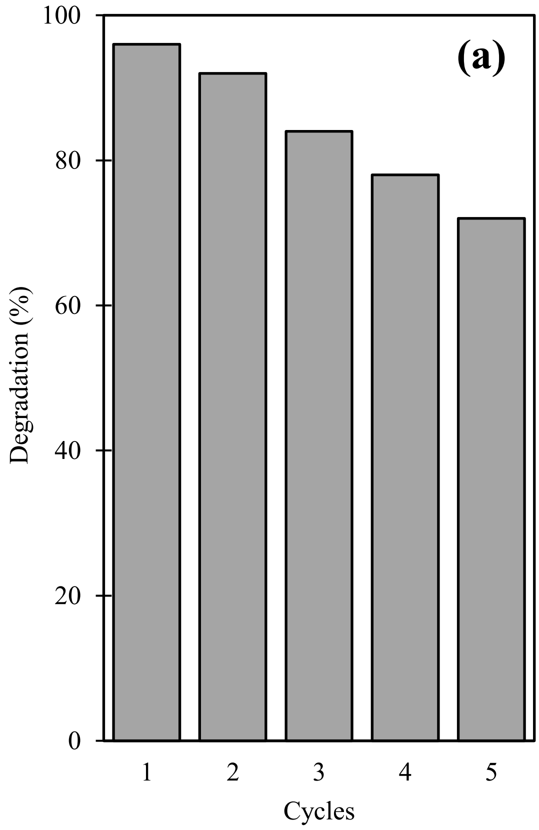

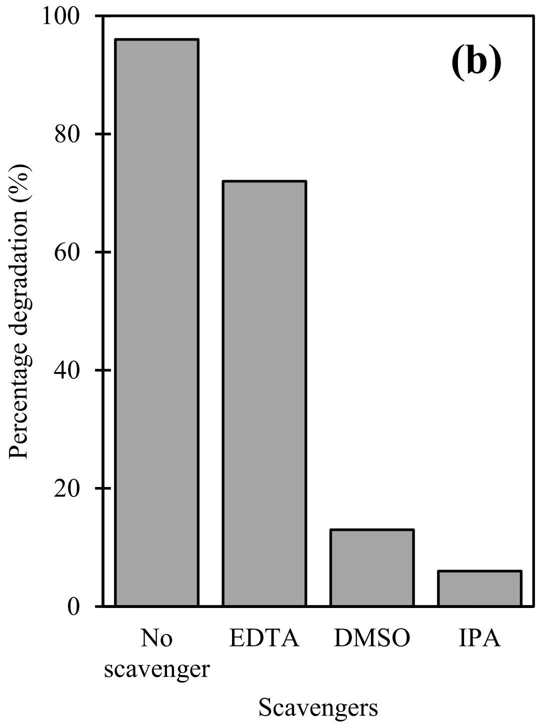

Fig. 6. (a) Reusability and (b) radical scavenging analysis of Z7A (condition: dosage = 0.1 g, PCM concentration = 20 ppm, time = 180 min, and pH = 6)

3.7 Performance comparison

Comparing Z7A with previously reported studies of using green synthesis technique revealed that waste-based material via BPE in ZnO-Ag synthesis has better potential in photocatalytic degradation application with high efficiency as shown in Table 1. As indicated, most previous studies use dye as model pollution and plant or fruit extract as green sources. Hence, Z7A is more promising for being used as a waste-based photocatalyst for removal of pharmaceutical pollutants.

Table 1. Performance comparison of green synthesized ZnO/Ag for photocatalytic degradation application

Green sources	Pollutant concentration	Degradation (%)	References
Oak fruit hull	Basic violet 3 (5 mg/L)	79	[33]
Tamarindus indica	Methylene blue (10 mg/L)	94	[34]
Acacia arabica	Methylene blue (15 mg/L)	90	[19]
Pedalium murex L.	Methylene blue (20 mg/L)	92.43	[15]
Banana peels	Paracetamol (20 mg/L)	96	This study

4 Conclusion

Banana peels based ZnO NPs and ZnO/Ag NPs were successfully synthesized via sol-gel and co-precipitation techniques. The formation of ZnO NPs and ZnO/Ag NPs shows a blue shift phenomenon indicating hybrid interaction between ZnO NPs and Ag NPs. XRD analysis shows similar peaks for all samples with ZnO hexagonal wurtzite structure and Ag component in Z5A and Z7A. The FESEM analysis shows Z7A portraited spherical and hexagonal shape and mesoporous structure. Among all samples, Z7A shows highest PCM degradation of 96 % with suitable dosage of 0.1 g of photocatalyst. Five repeated cycles with more than 60 % degradation of PCM was achieved through reusability analysis while the main species in PCM degradation via Z7A were ·OH and e^-.

The Ministry of Higher Education is sincerely thanked by the authors for providing funding for this project through the Grant Scheme of Fundamental Research Grant Scheme (FRGS/1/2020/STG05/UTM/02/9) (R.K130000.7843.5F403). Additionally, the authors express their gratitude for the financial support received from UTM Fundamental Research Grant (Q.K130000.3843.22H72). The authors also acknowledge with gratitude the utilization of services and facilities at Malaysia-Japan International Institute of Technology (MJIIT), Universiti Teknologi Malaysia and University of Tsukuba, Japan.

References

1. H.K. Paumo, S. Dalhatou, L.M. Katata-Seru, B.P. Kamdem, J.O. Tijani, V. Vishwanathan, A. Kane, I. Bahadur, TiO_2 assisted photocatalysts for degradation of emerging organic pollutants in water and wastewater. J. Mol. Liq. **331**, 115458 (2021).
2. J. Margot, L. Rossi, D.A. Barry, C. Holliger, A review of the fate of micropollutants in wastewater treatment plants. Wiley Interdiscip. Rev.: Water **2**, 457 (2015)
3. E.D. Mohamed Isa, K. Shameli, H.J. Ch'ng, N.W. Che Jusoh, R. Hazan, Photocatalytic degradation of selected pharmaceuticals using green fabricated zinc oxide nanoparticles. Adv. Powder Technol. **32**, 2398 (2021)
4. R. Sabouni, H. Gomaa, Photocatalytic degradation of pharmaceutical micro-pollutants using ZnO, Environ. Sci. Pollut. Res. Int. 26, 5371 (2019)
5 A.R. Lado Ribeiro, N.F.F. Moreira, G. Li Puma, A.M.T. Silva, Impact of water matrix on the removal of micropollutants by advanced oxidation technologies. Chem. Eng. J. **363**, 155 (2019)
6. N. Nassiri Koopaei, M. Abdollahi, Health risks associated with the pharmaceuticals in wastewater. DARU J. Pharm. Sci. **25**, 9 (2017)
7. E.C. Umejuru, E. Prabakaran, K. Pillay, Coal fly ash decorated with graphene oxide-tungsten oxide nanocomposite for rapid removal of Pb^{2+} ions and reuse of spent adsorbent for

photocatalytic degradation of acetaminophen. Acs Omega **6**, 11155 (2021)
8. A.-M. Abdel-Wahab, A.-S. Al-Shirbini, O. Mohamed, O. Nasr, Photocatalytic degradation of paracetamol over magnetic flower-like TiO_2/Fe_2O_3 core-shell nanostructures, J. Photochem. Photobiol. A **347**, 186 (2017).
9. K.S. Namshah, R.M. Mohamed, WO_3–TiO_2 nanocomposites for paracetamol degradation under visible light. Appl. Nanosci. **8**, 2021 (2018) 2021-2030.
10. P. Jayasree, N. Remya, Photocatalytic degradation of paracetamol using aluminosilicate supported TiO_2. Water Sci. Technol. 82, 2114 (2020)
11. T. Velempini, E. Prabakaran, K. Pillay, Recent developments in the use of metal oxides for photocatalytic degradation of pharmaceutical pollutants in water—a review. Mater. Today Chem. **19**, 100380 (2021).
12. C.A. Aguilar, C. Montalvo, B.B. Zermeño, R.M. Cerón, J.G. Cerón, F. Anguebes, M.A. Ramírez, Photocatalytic degradation of acetaminophen, tergitol and nonylphenol with catalysts TiO2/Ag under UV and Vis light. Int. J. Environ. Sci. Technol. **16**, 843 (2018)
13. C. Alberoni, I. Barroso-Martin, A. Infantes-Molina, E. Rodriguez-Castellon, A. Talon, H.G. Zhao, S.J. You, A. Vomiero, E. Moretti, Ceria doping boosts methylene blue photodegradation in titania nanostructures. Mater. Chem. Front. **5**, 4138 (2021)
14. Z. Noohpisheh, H. Amiri, S. Farhadi, A. Mohammadi-gholami, Green synthesis of Ag-ZnO nanocomposites using Trigonella foenum-graecum leaf extract and their antibacterial, antifungal, antioxidant and photocatalytic properties. Spectrochim. Acta - A: Mol. Biomol. **240**, 118595 (2020)
15. S. Mangala Nagasundari, K. Muthu, K. Kaviyarasu, D.A.A. Farraj, R.M. Alkufeidy, Current trends of Silver doped Zinc oxide nanowires photocatalytic degradation for energy and environmental application. Surf. Interfaces **23**, 100931 (2021)
16. S. Harinee, K. Muthukumar, R.A. James, M. Arulmozhi, H.U. Dahms, M. Ashok, Bio-approach ZnO/Ag nano-flowers: enhanced photocatalytic and photoexcited anti-microbial activities towards pathogenic bacteria. Mater. Today Sustain. **18**, 100133 (2022)
17. B.Y. Sahyar, M. Kaplan, M. Ozsoz, E. Celik, S. Otles, Electrochemical xanthine detection by enzymatic method based on Ag doped ZnO nanoparticles by using polypyrrole. Bioelectrochemistry **130**, 107327 (2019)
18. B. Ramasamy, J. Jeyadharmarajan, P. Chinnaiyan, Novel organic assisted Ag-ZnO photocatalyst for atenolol and acetaminophen photocatalytic degradation under visible radiation: performance and reaction mechanism. Environ. Sci. Pollut. Res. **28**, 39637 (2021)
19. M.J. Khan, K. Tahir, A.A. El-Zahhar, A. Arooj, H.A. Al-Abdulkarim, E.A.M. Saleh, S. Nazir, H.S. Al-Shehri, K. Husain, A.U. Khan, Facile synthesis of silver modified zinc oxide nanocomposite: An efficient visible light active nanomaterial for bacterial inhibition and dye degradation. Photodiagnosis Photodyn. Ther. **36**, 102619 (2021)
20. M. Ahmad, M.T. Qureshi, W. Rehman, N.H. Alotaibi, A. Gul, R.S. Abdel Hameed, M.A. Elaimi, M.F.H. Abd el-kader, M. Nawaz, R. Ullah, Enhanced photocatalytic degradation of RhB dye from aqueous solution by biogenic catalyst Ag@ZnO, J. Alloys Compd. **895**, 162636 (2022)
21. J. Kadam, P. Dhawal, S. Barve, S. Kakodkar, Green synthesis of silver nanoparticles using cauliflower waste and their multifaceted applications in photocatalytic degradation of methylene blue dye and Hg^{2+} biosensing, SN Appl. Sci. **2**, 738 (2020)
22. M.A.M. Mokhtar, Ali, R. R., Lei, Z., Jusoh, N. W. C., & Tarmizi, Z. I. A, Efficiency of Low-Ag-content biosynthesized ZnO/Ag on photodegradation of paracetamol. Chem. Eng. Trans. **106**, 1051 (2023)
23. H.D. Kyomuhimbo, I.N. Michira, F.B. Mwaura, S. Derese, U. Feleni, E.I. Iwuoha, Silver–zinc oxide nanocomposite antiseptic from the extract of Bidens pilosa, SN Appl. Sci. 1 (2019) 681.
24. Y.S. Jung, J. Wuenschell, H.K. Kim, P. Kaur, D.H. Waldeck, Blue-shift of surface plasmon resonance in a metal nanoslit array structure. Opt Express **17**, 16081 (2009)
25. R. Singh, P.B. Barman, D. Sharma, Synthesis, structural and optical properties of Ag doped ZnO nanoparticles with enhanced photocatalytic properties by photo degradation of organic dyes. J. Mater. Sci.: Mater. Electron. **28**, 5705 (2017)
26. K.R. Basavalingiah, S. Harishkumar, Udayabhanu, G. Nagaraju, D. Rangappa, Chikkahanumantharayappa, Highly porous, honeycomb like Ag–ZnO nanomaterials for enhanced photocatalytic and photoluminescence studies: green synthesis using Azadirachta indica gum. SN Appl. Sci. **1**, 935 (2019)
27. F.H. Abdullah, N.H.H. Abu Bakar, M. Abu Bakar, Low temperature biosynthesis of crystalline zinc oxide nanoparticles from Musa acuminata peel extract for visible-light degradation of methylene blue. Optik **206**, 164279 (2020)
28. D. Thatikayala, N. Jayarambabu, V. Banothu, C.B. Ballipalli, J. Park, K.V. Rao, Biogenic synthesis of silver nanoparticles mediated by Theobroma cacao extract: enhanced antibacterial and photocatalytic activities. J. Mater. Sci.: Mater. Electron. **30**, 17303 (2019)
29. Z. Shaghaghi, S. Mollaei, A.R. Amani-Ghadim, Z. Abedini, Green synthesis of ZnO nanoparticles using the aqueous extract of Platanus orientalis: Structural characterization and photocatalytic activity. Mater. Chem. Phys. **305**, 127900 (2023)

30. M. Thommes, K. Kaneko, A.V. Neimark, J.P. Olivier, F. Rodriguez-Reinoso, J. Rouquerol, K.S.W. Sing, Physisorption of gases, with special reference to the evaluation of surface area and pore size distribution (IUPAC Technical Report). Pure Appl. Chem. **87**, 1051 (2015)
31. F.H. Abdullah, N.H.H. Abu Bakar, M. Abu Bakar, Comparative study of chemically synthesized and low temperature bio-inspired Musa acuminata peel extract mediated zinc oxide nanoparticles for enhanced visible-photocatalytic degradation of organic contaminants in wastewater treatment. J. Hazard. Mater. **406**, 124779 (2021)
32. M.A. Al-Gharibi, H.H. Kyaw, J.N. Al-Sabahi, M.T. Zar Myint, Z.A. Al-Sharji, M.Z. Al-Abri, Silver nanoparticles decorated zinc oxide nanorods supported catalyst for photocatalytic degradation of paracetamol. Mater. Sci. Semicond. Process. **134**, 105994 (2021)
33. M. Sorbiun, E. Shayegan Mehr, A. Ramazani, S. Taghavi Fardood, Biosynthesis of Ag, ZnO and bimetallic Ag/ZnO alloy nanoparticles by aqueous extract of oak fruit hull (Jaft) and investigation of photocatalytic activity of ZnO and bimetallic Ag/ZnO for degradation of basic violet 3 dye. J. Mater. Sci.: Mater. Electron. **29**, 2806 (2018)
34. D. Thatikayala, V. Banothu, J. Kim, D.S. Shin, S. Vijayalakshmi, J. Park, Enhanced photocatalytic and antibacterial activity of ZnO/Ag nanostructure synthesized by Tamarindus indica pulp extract, J. Mater. Sci.: Mater. Electron. **31**, 5324-5335 (2020).